International Journal of Heat and Mass Transfer 159 (2020) 120099

Contents lists available at ScienceDirect

International Journal of Heat and Mass Transfer

journal homepage: www.elsevier.com/locate/hmt

Experimental study of the falling film evaporation coefficients of R290 in a horizontal enhanced tube array

Ibrahim Mostafa, Pu-Hang Jin, Zhuo Zhang, Wen-Quan Tao*

International Joint Research Laboratory of Thermal Science & Engineering, Xi'an Jiaotong University, Xi'an, Shaanxi 710049, China

ARTICLE INFO

Article history:
Received 15 January 2020
Revised 15 May 2020
Accepted 14 June 2020
Available online 9 July 2020

Keywords:
Falling film evaporation
Heat transfer performance
Tube array
Enhanced tube
R290

ABSTRACT

In this study, the falling film evaporation heat transfers of R290 on an array composed of five enhancement horizontal tubes (groove tubes) are studied. The tests are performed at constant saturation temperatures 5.5 °C with change of heat flux from 10 to 40 kW/m^2. The film Reynolds number ranges from 200 to 2200 and the film flow rate of refrigerant is between 100 and 660 kg/h.

The results show that the film flow rate and heat flux have significant effects on R290 falling film evaporation heat transfer coefficients (HTCs) of the tubes in the tube array. With decreasing the film flow rate on the five tubes the tube HTCs display two stages, a plateau stage and a sharp drop stage. The heat transfer coefficients firstly keep more or less constant at the plateau stage and then decreasing rapidly. At the same nominal film Reynolds number the tube averaged heat transfer coefficients of tube No. 1 to tube No. 5 decrease in order of the increasing tube number from top to bottom of the array. The falling film evaporation HTC of R290 on single enhanced tube is about 4.5 times of single smooth tube HTC, and the HTCs of the enhanced tube array is higher than single smooth tube by more than 2.5 times. In addition, the R290 HTCs of the tube array are higher than those of R134a for the same tube array in the plateau region by about 25%. It is found that at high heat flux of 30–40 kW/m^2, the heat transfer coefficient variation with film Reynolds number of the lower enhanced tubes in the tube array exhibits severe undulating characteristics.

1. Introduction

Falling film evaporators have been widely employed in a large number of industrial processes, such as petrochemical industry, desalination processes, OTEC (ocean thermal energy conversion) systems, food and dairy industries, etc. [1].

In the past decades, the application of falling film evaporation outside the horizontal tube in the large refrigeration and air-conditioning systems attracted great attentions. Many researches have indicated that this technology is a potential alternative to the flooded evaporation due to its superiorities of less refrigerant charge, higher heat transfer coefficient, negligible static pressure difference and easier lubrication return. However, the design of falling film evaporator is extremely complicated because of the complexities of the fluid flow and heat transfer process.

As the global warming has raised more critical concerns in recent years, refrigerants, such as R22, R410A and R134a with high global warming potential (GWP), are facing the challenge of being phased out. Hydrocarbons, such as R290, R600a, and R1233zd have a zero ozone depletion potential (ODP) and an extremely low GWP, have attracted research interests in heat transfer community, even though their safety performance needs further investigation.

Flooded evaporators have been used in desalination and dairy industries for several decades. The most disadvantage of the flooded evaporator is its large charged amount of refrigerant. This character is especially unfavorable when the used refrigerant is not friendly to the environment. In addition, the large charge amount of refrigerant is a big thermal inertia which makes the flooded evaporator being slow response to transient operation. In the contrast, the falling film evaporators in general, are highly responsive to operational parameters, such as energy supply, pressure levels and feed rate. The fact that falling film evaporators can be operated with small temperature differences makes them allowable to the application in multiple effect configurations.

A schematic picture of the falling film evaporator is shown in Fig. 1. When a liquid, under the influence of gravity, flows from a distributor and down to the tubes below, evaporation of the liquid refrigerant occurs on tube surface. The flow may take different forms dependent on the tube arrangement and relative magnitudes of applied forces.

* Corresponding author.
E-mail address: wqtao@mail.xjtu.edu.cn (W.-Q. Tao).

https://doi.org/10.1016/j.ijheatmasstransfer.2020.120099
0017-9310/

Nomenclature

A	area, m^2
c_p	specific heat capacity, J kg^{-1} K^{-1}
D	diameter of tube, mm
g	gravity acceleration, m s^{-2}
h	heat transfer coefficient/HTC, W m^{-2} K^{-1}
k	overall heat transfer coefficient, W m^{-2} K^{-1}
L	test length of tube, mm
$\dot{m}$	mass flow rate, kg s^{-1}
q	heat flux, kW m^{-2}
Q	heat transfer rate, W
R	thermal resistance, m^2KW^{-1}
Re	film Reynolds number
T	temperature,°C
Greek	
Γ	liquid film flow rate on one side of the tube per unit length, kg m^{-1} s^{-1}
ϕ	heat transfer rate, W
μ	dynamic viscosity, kg m^{-1} s^{-1}
ρ	density, kg m^{-3}
Subscript	
ave	average variable
c	condensing
e	evaporating
LMTD	logarithmic mean temperature difference
i	inside of tube
o	outside of tube
sat	saturation
w	wall

Falling film flow is affected by gravitational force, viscous force and surface tension. Depending on the relative importance of the three effects, the liquid flowing through a tube bundle may form three basic modes shown in Fig. 2. These are: (a) the droplet mode, (b) the column mode and (c) the sheet mode [2].

To reveal the heat transfer performance of falling film evaporation on single tube and tubed banks, many researches have been done. The major results published before 2005 have been reviewed by Ribatski and Jacobi in [1] and will not be restated here. A brief summary on the falling film evaporation of refrigerants on single tube or tube banks since 2005 is shown in Table 1 for the simplicity of presentation.

From the table, it can be seen that the only experimental study for R290 has been carried out for the new refrigerants R290 is for single smooth tube, and there is no any test data for R290 on enhanced tube array.

In the following presentation, the test setup and procedure will be provided first (Section 2), followed by the data reduction method (Section 3). Then the test results are presented and discussed (Section 4). Finally some conclusions are drawn in Section 5.

2. Experimental setup and procedure

2.1. Test system

An experimental setup was built to investigate falling film evaporation on tube bundles which can work in a vacuum state or pressurized state. The schematic diagram of test system is shown in Fig. 3. The experimental setup is comprised of three liquid forced-circulation loops: the working fluid (refrigerant) circuit, the heating water circuit of evaporator and a cooling water circuit of condenser. The heating water flowing inside several parallel horizontal tubes provides the heat for refrigerant film evaporation outside the tubes. The cooling water condenses the refrigerant vapor on the other side of the condenser vessel. The refrigerant circuit contains a condenser (1) and the test section (evaporator) (2). The evaporator is a circular stainless-steel vessel with windows situated at the middle in order to have visual access to observe the flow on the tubes.

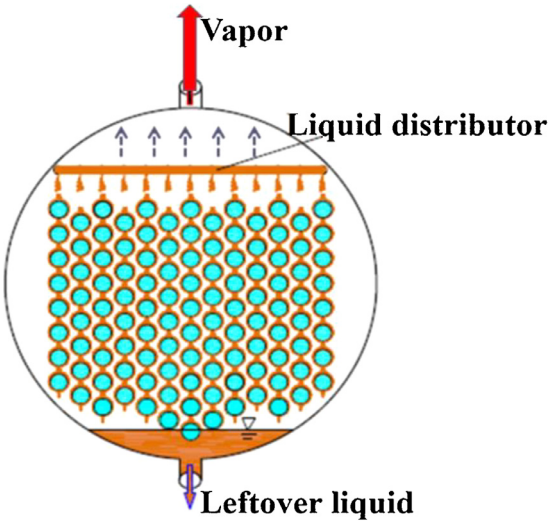

Fig. 1. Configuration of horizontal tube falling film evaporator.

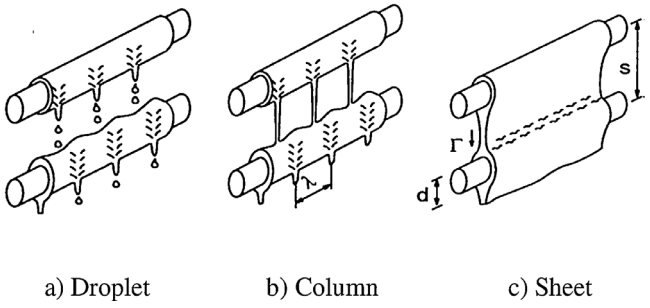

Fig. 2. Three falling film patterns [1].

Liquid distributor used in this test is shown in Fig. 4. It is comprised of two rectangular boxes, and they separately serve as a preliminary and a secondary distributor which are in vertical line with the top-most points of the tested tubes. The top plate of the second one is open-ended. Orifices with diameter of 2.0 mm and spacing of 15.0 mm were drilled at the bottom surface of the second box. With the same diameter and pitch, two rows of orifices were drilled at the bottom plate of top box. The distance is 6 mm between the bottom surface of the distributor and the dummy tube above the tube bundle. The function of the 1st box is to approximately unify the along-tube-axis distribution of the liquid which drops down on the second box. In the second box the refrigerant forms a liquid pool with a height varying with flow rate and further falls down to the top tube of the bundle under the action of gravity.

A cross-sectional schematic of the tube bundle is shown in Fig. 5. The top tube is a dummy one. Single enhanced tube and a five-tube bundle were tested in our experiments. The distance between the dummy tube and the first test tube is 25.4 mm and the pitch of the other tubes is also fixed at 25.4 mm. The tubes tested are enhanced copper tube with the same specifications. The enhanced tube has outer diameter of 18.86 mm, inner diameter of

Table 1
Summary of research works on refrigerant falling film evaporation since 2005.

Authors	Working fluid	Tube	T_{sat} (°C)	D_o (mm)	Heat Flux (kW/m^2)	Main results
Ribatski and Jacobi [1]	Review paper					The basic mechanisms responsible for falling film evaporation heat transfer are still unclear. The HTCs of the enhanced tubes is undermined by complicated heat transfer dependence on geometry, tube layout, and operating conditions. Bundle depth effects related to liquid maldistribution and partial dry-out still unclear. In addition, liquid distribution has a dramatic effect on evaporator performance.
Gstöhl And Thome [2]	R-134a	Vertical tube array with plain and enhanced surfaces under adiabatic test conditions (plain tube/Turbo-Chil/Turbo-CSL/Gewa-C)	Room temperature for flow pattern visualization	18.88–18.91-18.94	/	With an increasing film Reynolds number of refrigerant, the observed flow modes were: droplet mode, droplet-column mode, column mode, column sheet mode, and sheet mode. The ideal flow modes could only be observed on the 3D-enhanced tubes. The influence of tube spacing was found to be of minor importance on the observed flow patterns.
Habert and Thome [3,4]	R134a and R236fa	Tube bundle (plain, enhanced condensing, enhanced boiling)	5	19.05	20–40–60	The HTCs are strongly dependent on the heat flux. The flow on the tubes to be a thick bubble layer, not a thin liquid film. In a bundle configuration, different trends were observed depending of the type of tube, but bundle effects were quite obvious with regard to the single-row test results. New prediction methods were proposed. Appreciable fluctuation of HTCs are observed.
Roques and Thome [5]	R-134a	Arrays of horizontal tubes (plain, Turbo-BII HP, Gewa-B, and High-Flux tubes)	5	18.91- 18.84-18.87	25–34–40–70–80	A new method for determining local heat transfer coefficients using hot water heating has been implemented, and the HTCs have been measured for arrays made of plain and four enhanced tubes. Vigorous nucleate boiling is always seen in the liquid film.
Roques and Thome [6]	R-134a	Arrays of Horizontal Tubes (plain, Turbo-BII HP, Gewa-B, and High-Flux tubes)	5	18.91- 18.84-18.87	25–34–40–70–80	The film Reynolds number at the onset of dryout is a strong function of heat flux. The HTCs above the onset of dryout threshold are nearly insensitive to the film Reynolds number. A new empirical method has been proposed to describe falling film heat transfer on plain and enhanced tubes when nucleate boiling dominates. It predicts their test data of falling film heat transfer coefficients to within ±20%.
Chien and Tsai [7]	R-245fa	Horizontal copper tubes, smooth tub, fin tube	5–20	19	6–12–37–50	The boiling enhanced tube (mesh tube) yielded a higher falling film vaporization HTC than the fin tube in R-245fa, but it was inferior to the fin tube in R-134a. The mesh tube and the (60 FPI) fin tube enhance the heat transfer coefficient up to 5.0 fold and 3.5 fold, respectively, compared with the smooth tube. R-245fa results in slightly higher HTCs in falling film vaporization than R-123.New correlations of horizontal smooth tube are proposed.
Christians and Thome [8]	R-134a and R-236fa	Single tube, Tube bundle, enhanced boiling tubes (Wolverine Turbo-B5 and the Wieland Gewa-B5)	5	19.05	15 to 90	No additional bundle effects could be found when testing in bundle configuration compared with single array tests. R-134a outperforms R-236fa for the enhanced tube tested which was designed for R134a in pool boiling. However, the degradation is smaller when testing in falling film than in pool boiling.
Christians and Thome [9]	R-134a and R-236fa	Single tube, tube bundle, enhanced boiling tubes (Wolverine Turbo-B5 and the Wieland Gewa-B5)	5–10–15	19.05	15 to 90	The previous experimental data of the authors group were utilized to generate new predictive methods for the onset-of-dryout for falling film evaporation, and the plateau heat transfer coefficient. For the partially dry heat transfer coefficient prediction $h_{partialdo} = Fh_{plateau}$ is put forward, where F is the fraction of wetted surface area.
Fernández-Seara and Pardiñas [10]	Review for refrigerant falling film evapora-tion					Main parameter of Falling film evaporator are heat flux, film flow rate, geometry of the tube, refrigerant properties and distribution system. The enhanced tubes improve falling film HTCs compared by the plain tubes. Most enhanced tubes delay film breakdown, maintaining the surface wet. The accuracy of the developed correlations is normally limited to very specific experimental conditions.
Ji et al. [11]	R134a	Tube bundle	6	19.05	20–40–60	Effect of vapor flow on the falling film evaporation of R134a outside a horizontal tube bundle was studied. The impact of vapor flow, both positive and negative effects are observed as the increasing of vapor velocity. Positive effects are predominant for the two tubes in the top at higher vapor velocity.

(*continued on next page*)

Table 1 (*continued*)

Authors	Working fluid	Tube	T_{sat} (°C)	D_o (mm)	Heat Flux (kW/m^2)	Main results
Zhao et al. [12]	R134a	Single horizontal smooth tube	6–10–16	16.0- 19.05-25.35	20–40–60–80	The influence of tube diameter on heat transfer may be positive or negative depending on the levels of the heat flux and film flow rate. The effect of saturation temperature on heat transfer is positive at lower heat flux while negative at higher heat flux. Two correlations for R134a falling film evaporation on single tune were constructed.
Zhao et al. [13]	R134a and R123	Smooth tube and four enhanced tubes	6	18.89–19.03–19.04–19.05–19.06	20–40–60	One smooth tube and four enhanced tubes were tested. The enhanced four tubes have 50,48,45 51 fins per inch respectively. R134a provides around 2–3 times of HTCs of those of R123 at the film flow rate region larger than 0.025 kgm^{-1}s^{-1}. At larger film flow rate the HTCs of R123 increase with heat flux for all tubes. For R134a, HTCs of Nos. 1, 3 and 4 increase with flux, while tube No.2 first increase then decrease.
Zhao et al. [14]	R134a	Enhanced tube bundle	6–10–16	19.05	20–40–60–80	Bundle depth is an important influencing factor on HTCs of each individual tube. With increase in bundle depth, the lower tubes exhibit poor heat transfer performances for the shortage of liquid. A higher saturation temperature improves the falling film evaporation. The average tube bundle coefficients decrease with heat flux but increase with saturation temperature. Some fluctuation of HTCs of the lower tubes can be identified.
Jin et al. [15]	R410A and R32	horizontal two-row enhanced tubes	6–10–16	19.06–19.04–19.03–18.89–19.05	20–40–60	For both refrigerants, HTCs increase with heat flux before reaching the partial dryout . The effect of saturation temperature on the enhanced tubes and tube bundle is negligible. The HTCs of R32 are larger than those of 410A. Tubes positioned in the second row suffer an earlier dryout because less flow rate supply compared with the upper ones.
Jin et al. [16]	R134a, R290 and R600a	Single smooth tube	6–10	19.05	10 to 60	The effect of heat flux on falling film evaporation heat transfer is always positive in both full wetting and partial dry-out regimes. HTC of R600a is inferior than R134a, while R290 is slightly higher than those of R134a.Two correlations of full-wetting and partial dry-out for five refrigerants are constructed for single smooth tube.
Jin et al. [17]	R134a	Enhanced tube bundles	5.5	18.86	10–20–30–40	The effect of film Reynolds number on tube HTCs varies with tube position in the tube bundle. For single tube the effect of heat flux on falling film evaporation heat transfer is positive at lower heat flux and negative at larger ones. The effect of heat flux on the bundle averaged HTC increases with tube pitch. The HTCs fluctuation starting from 3rd tube can be observed clearly.

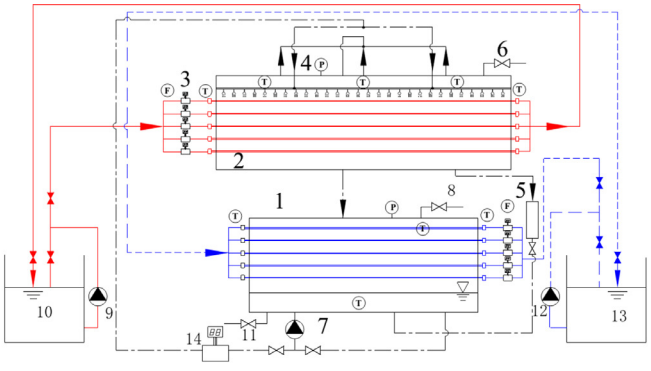

1. Condenser 2. Evaporator 3. Electromagnetic flowmeter 4. Pressure guage 5. Condenser measuring container 6. Exhausting valve 7. Refrigerant magnetic pump 8. Refrigerant charging valve 9. Heating water pump 10. Heating water tank 11. Refrigerant outlet 12. Cooling water pump 13. Cooling water tank 14. Refrigerant mass flow meter

Fig. 3. Schematic diagram of test system.

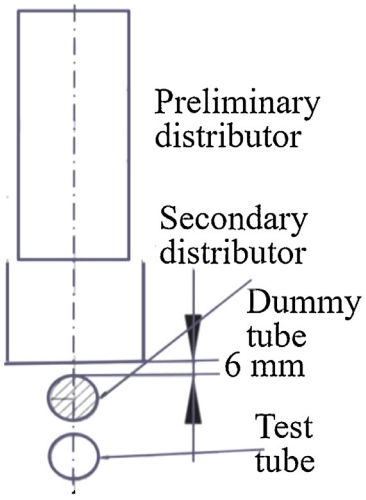

(a) Cross-section of liquid distributor

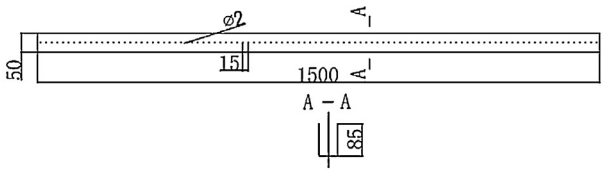

(b) Preliminary Liquid Distributor

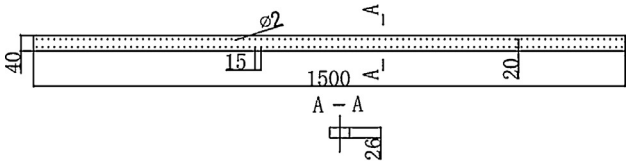

(c) Secondary Liquid Distributor

Fig. 4. Liquid distributor.

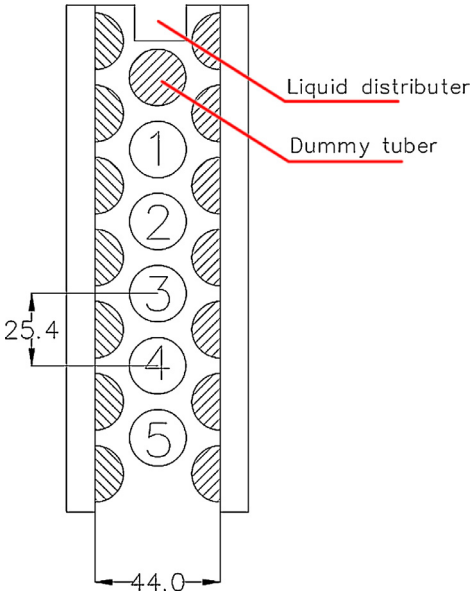

Fig. 5. Layout of tube array.

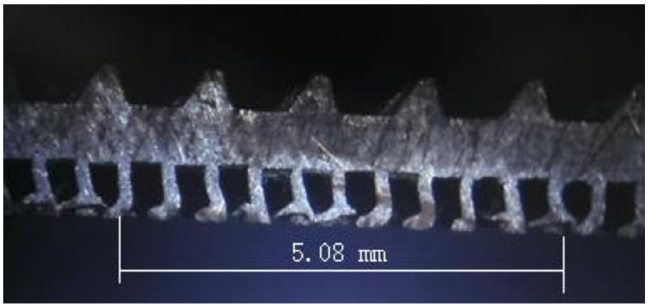

(a) Cross sectional view

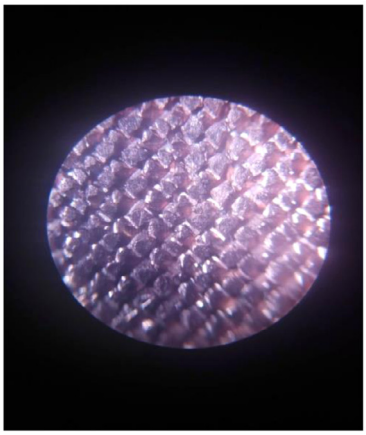

(b) Regional top view of tube surface

Fig. 6. Scanning pictures of the enhanced surface.

16.33 mm and effective length of 1500 mm. The fin density is 50 per inch.

The scanning pictures of the enhanced surfaces are shown in Fig. 6 where the scale of reference length is shown.

During the test run, the refrigerant liquid temperature and pressure of the test evaporator were measured simultaneously. A thermocouple was placed in the second box of the liquid distributor to measure the inlet liquid temperature. These measured liquid temperatures are in good agreement with the saturated temperatures correspondent to the measured pressure with a deviation 0.02 K.

Finally some information of the measurement methods and their accuracy are provided. The inlet and outlet temperatures of the heating water were measured by resistance temperature detectors (RTDs) Pt100. The outer diameter of the shell for the RTDs is 1 mm. The pressure in the evaporator was measured by a digital pressure gauge. Pressure transducers connected to the test section of evaporator on a top of array of tubes were used to measure the vapor pressure in the test section. Specifications of measurement instruments are listed in Table 2.

2.2. Experimental procedure

When the installations of the test section, flanges and insulation are completed, the high-pressure nitrogen is charged into the system until the internal pressure is about double times of the working pressure, and then the pressure is maintained for 72 h to ensure that there is no leak from the system. If the pressure change during this period is less than 1 kPa the nitrogen is drained, then a vacuum pump is connected to the system to remove all non-condensable gases, till the absolute pressure of the system is no

Table 2
Specifications of key measurement instruments.

Instruments	Specification	Precision	Range
Mass flow meter	SIEMENS MASS2100	0.1%	0–5000 kg.h^{-1}
Volume flow meter	SIEMENS MAGFLO MAG5100W	0.1%	0–3000 L.h^{-1}
Pressure gauge	KELLER LEX1	0.05%	−0.1 to 2.0 MPa
RTDs	OMEGA Pt100 1/10 DIN	± (0.03 + 0.0005[T]) °C	0–60 °C
Data acquisition	Keithley digital voltmeter	0.1 μV	1000 V

more than 800 Pa. Finally, a small amount of tested refrigerant is first charged and then the system is evacuated to the pressure 1 kPa again. This procedure is repeated three times, and then the refrigerant is charged with an appropriate amount of weight.

In the experimental procedure for the five vertical tube rows, all five tubes are cooled by in-tube water and their heat transfer performance is tested simultaneously. For the heat transfer test of the entire tube array, it is not possible to make all the five tubes having the same test condition because of the continuous evaporation of refrigerant from top tube to the bottom tube. Then the test parameters are adopted from the top tube and regarded as the test parameter of the entire tube bundle. In this experiment, the tested film Reynolds numbers range from 150 to 2100 and the heat fluxes are kept at four levels of 10, 20, 30 and 40 kW/m^2. These numbers are actual heat fluxes only for the first tube, and for other four tubes they are nominal ones. The heat flux is changed by adjusting the cooling water temperature and flow rate.

During the experiments, the RTD output signal, the film flow rate, and the surface heat flux were monitored continuously by a data-acquisition system (DAQ) and shown on the desktop computer. It usually takes approximately 30–60 min for the system to reach steady-state conditions (as indicated by a variation in the saturation temperature of less than 0.02 ^{0}C/5 min). Then each data point of interest was taken by averaging a minimum of 10 data-acquisition scans. Note that in the tests, the input power should be immediately shut down if any of the heater temperature measurements suddenly increasing, indicating the appearance of a severe dry-out, in order to protect the measurement instrumentations.

During the test, the temperature of cooling water tank was maintained between 4.5 ^{0}C and 5.5 ^{0}C and the temperature of heating water tank was maintained between 9.5 ^{0}C and 11 ^{0}C. And the evaporator pressure was maintained at about 1000 Pa.

3. Data reduction

The energy balance for the system is examined by the following two equations. Eqs. (1) and (2) represent heating power input from heating water and cooling power output from cooling water, respectively.

$$\phi_{e,m} = \dot{m}_{e,m} C_{p,m} (T_{e,m,in} - T_{e,m,out}) \tag{1}$$

$$\phi_{c,n} = \dot{m}_{c,n} C_{p,n} (T_{c,n,out} - T_{c,n,in}) \tag{2}$$

where $T_{e,m,in}$ and $T_{e,m,out}$ represent the temperature of inlet and outlet of the hot water through each tube of the evaporator, respectively, $T_{c,n,in}$ and $T_{c,n,out}$ represent the temperature of inlet and outlet cold water through the tubes of condenser, respectively, $\dot{m}_{e,m}$ and $\dot{m}_{c,n}$ denote the mass flow rate of heating and cooling water, respectively, and $c_p$is the specific heat capacity of water inside each tube. The properties of water are obtained from [18].

For all the test data presented in this paper, heat balance deviation of the system is less than 5%, defined by the following equation:

$$\left(\sum_{m=1}^{M} \phi_{e,m} + \phi_p - \sum_{n=1}^{N} \phi_{c,n} \right) / \phi_a \le 5\% \tag{3}$$

where M and N are tube numbers in evaporator and condenser, respectively.

In Eq. (5) $\phi_a = 0.5 \left(\sum_{m=1}^{k} \phi_{e,m} + \sum_{n=1}^{1} \phi_{c,n} \right) + \phi_p$ is the heat transfer rate of tube bundle and the ϕ_p is the power of the canned motor pump which is immersed in the liquid refrigerant for pumping the liquid refrigerant in the condenser to the liquid distributor.

The overall heat transfer coefficients of the tested tube can be calculated by the following equation:

$$k_m = \frac{\phi_{e,m}}{A_{o,m}\ \Delta T_{LMTD}} \tag{4}$$

where $A_{o,m}$ is the nominal outer surface area of the tube, and ΔT_{LMTD} is the log-mean temperature difference between water and refrigerant saturation temperature for each test tube, which is defined by the following equation:

$$\Delta T_{LMTD} = \frac{T_{e,in} - T_{e,out}}{\ln\left(\frac{T_{e,in} - T_{sat}}{T_{e,out} - T_{sat}} \right)} \tag{5}$$

where T_{sat} is the saturation temperature of the refrigerants.

The overall thermal resistance of each tube can be written as the following equation:

$$\frac{1}{k_m} = \frac{1}{h_{i,m}} \frac{D_{o,m}}{D_{i,m}} + \frac{1}{h_{o,m}} + R_{w,m} \tag{6}$$

where D_i and D_o represent the internal and external diameter, respectively, h_i is the internal convection heat transfer coefficient, and R_w is the thermal resistance of the tube wall.

Therefore, the falling film evaporation heat transfer coefficient can be expressed as the following equation:

$$\frac{1}{h_{o,m}} = \frac{1}{k_m} - \frac{1}{C_{i,m}\ h_{gni,m}} \frac{D_{o,m}}{D_{i,m}} + R_{w,m} \tag{7}$$

where $h_{gni,m}$ is calculated from Gnielinski equation [19] and C_i represent the internal enhanced factor, which is determined by Wilson method [18,20].

The film Reynolds number of the film flow is determined by the following equation:

$$Re = \frac{4\Gamma}{\mu_l} \tag{8}$$

where Γ represents the single side film flow rate on the tested top tube per unit length, and μ_l represent the dynamic viscosity of the liquid refrigerant at the specific saturation temperature.

During the test, when q_o = 10 kW/m^2 the water flow rate was reduced to 1 m/s (Re~12,000 is within the applicability of Gnielinski equation) to meet the requirement that the minimum temperature difference at least 1 °C; while for other cases of higher heat fluxes from 20 to 40 kW/m^2, the minimum water temperature difference was kept around 2 °C.

The uncertainty analysis of the present data was conducted with the method presented in [21,22], and it was adopted in several our previous studies, such as [20]. Here, the uncertainty of h_i predicted by the Gnielinski equation is taken as 10% [23]. The estimated uncertainty of k is equal to or less than 5% for all the test points, and the uncertainty of falling film evaporation heat transfer coefficient h_o is estimated within ± 25%.

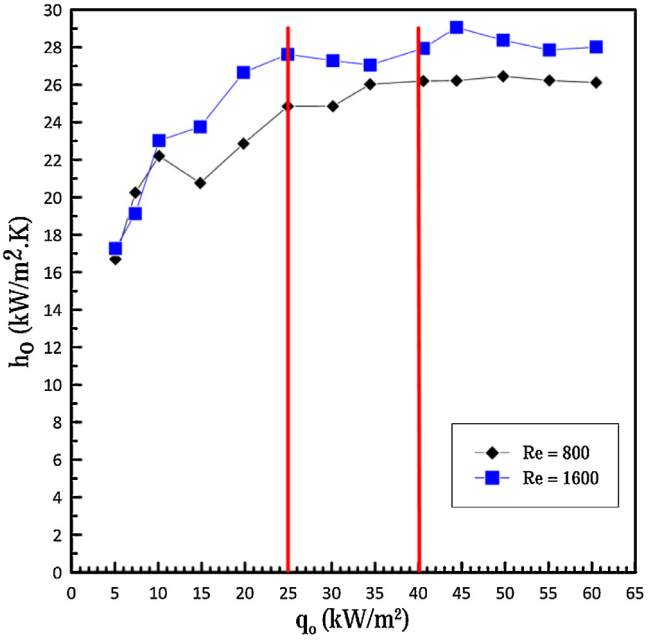

Fig. 7. Falling-film evaporation on tube No. 2 at heat flux from 5 to 60 kW/m^2.

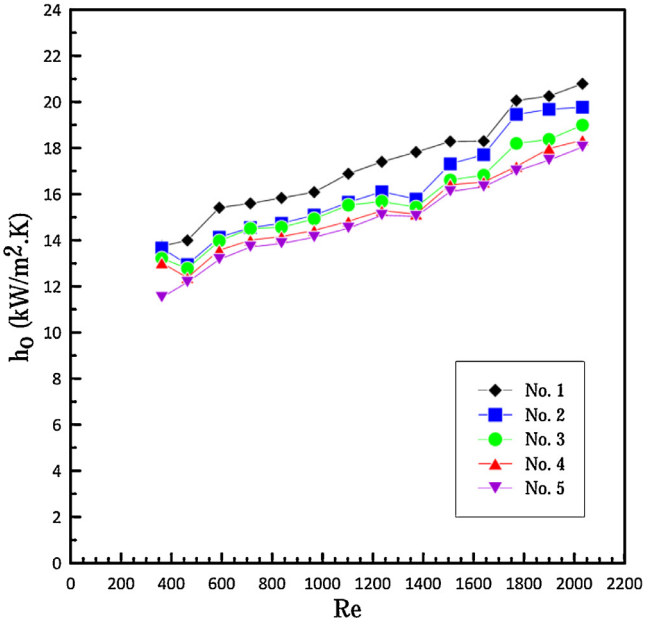

Fig. 8. Falling-film evaporation on enhancement tube array with R290 at 10 kW/m^2.

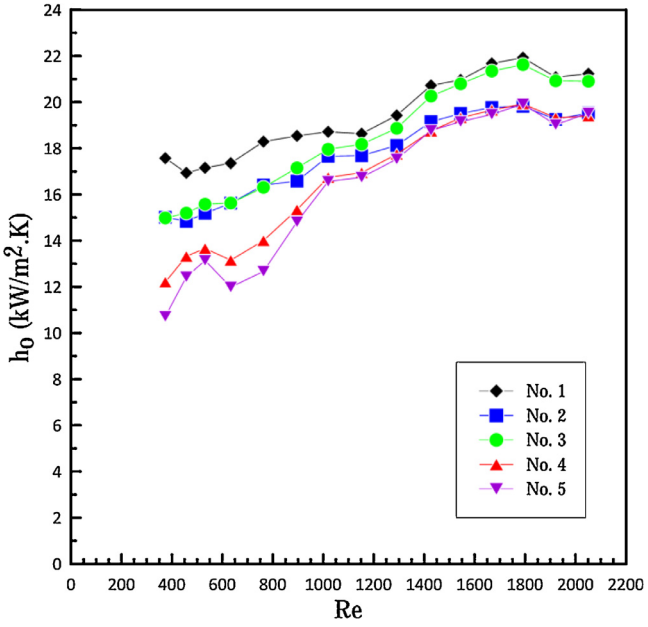

Fig. 9. Falling-film evaporation on enhancement tube array with R290 at 20 kW/m^2.

4. Results and discussion

Effects of film Reynolds number and heat flux on heat transfer performance will show in this section. The test was implemented at saturation temperature is 5.5 ^{0}C. First, for tube No. 2, heat transfer coefficients at heat flux varied from 5 to 60 kW/m^2 with two films Reynolds number (800 and 1600) were measured. Then the entire tube bank test was conducted with four nominal heat fluxes of 10, 20, 30 and 40 kW/m^2. For every heat flux, around twelve different overfeed rates onto the top tube of the array were tested. These overfeed rates are between 120 and 660 kg/h.

4.1. Reliability validation of the measurement system

Even though a large number of test data have been obtained from our test system [11–17], before the data run for R290 falling film evaporation, the measurement system was once again checked by condensation heat transfer of the refrigerant R 290 on a single tube, and good agreement was obtained between measured HTCs and those predicted by Nusselt theory, with ± 10 percentage of deviation, indicating the reliability of the test system.

4.2. Single enhanced tube test

The variation trend of h_o versus q for tube No. 2 under two films Reynolds numbers at saturation temperature of 5.5 ^{0}C is presented in Fig. 7. When tube No. 2 was in test, all other four tubes were kept idle that no heating water going through these tubes.

Three regimes can be clearly observed which are separated by two vertical lines at heat flux of 25 kW/m^2 and 40 kW/m^2, respectively. Heat transfer coefficient increases sharply with heat flux in the region below 25 kW/m^2, which is the indication that boiling heat transfer boiling heat transfer is important because pool boiling heat transfer coefficient increases with heat flux (usually $h_o \propto q^{0.6}$). In addition the heat transfer coefficient also increases appreciably with film Reynolds number. Therefore in this heat flux region both single-phase convective and boiling heat transfer play their roles. Then in the region between 25 kW/m^{2}and 40 kW/m^2, the heat transfer coefficient increases mildly with heat flux, while it still increases with the film Reynolds number. This implies that in this region boiling heat transfer mechanism plays less important role and convective heat transfer is important. Beyond that, the heat transfer coefficient almost keeps constant. This variation trend of h_o vs. q at different film Reynolds numbers shows that for the enhanced tube studied at region of high heat fluxes (more than 40 kW/m^2) nucleate boiling heat transfer plays a limited role and convective heat transfer mechanism is dominated.

4.3. Tube array test

The results for tube array are presented in Figs. 8–11 for nominal heat fluxes of 10, 20, 30, and 40 kW/m^2, respectively. The tested film Reynolds number ranges from 400 to 2000.

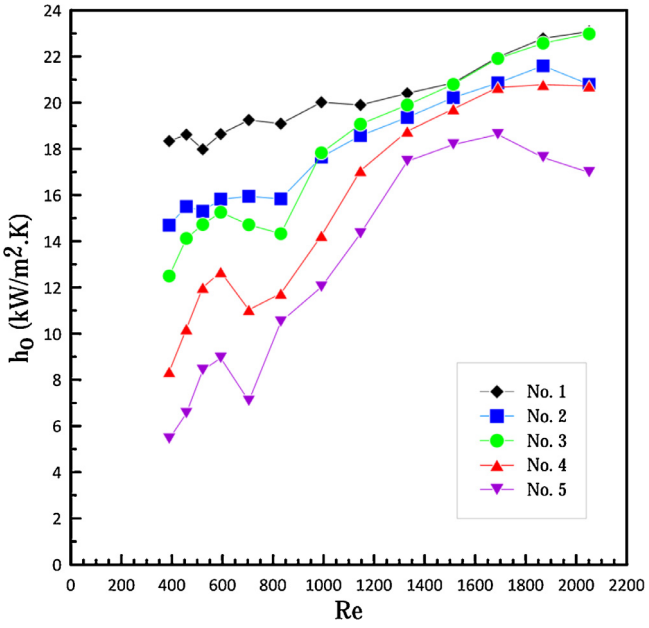

Fig. 10. Falling-film evaporation on enhancement tube array with R290 at 30 kW/m^2.

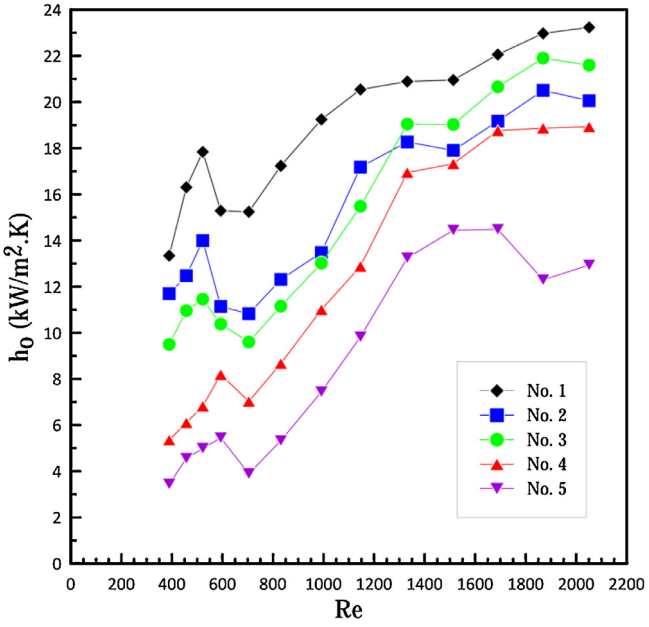

Fig. 11. Falling-film evaporation on enhancement tube array with R290 at 40 kW/m^2.

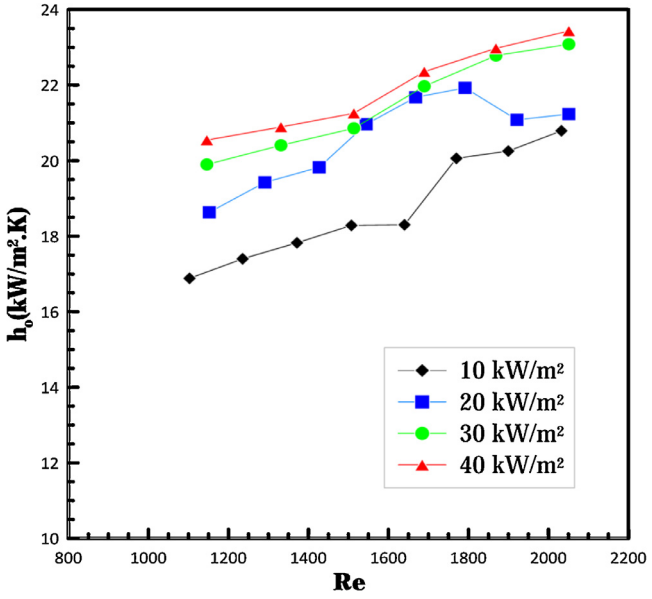

Fig. 12. Falling-film heat transfer coefficients of enhanced tube No. 1 versus film Reynolds number at different heat fluxes.

From Figs. 8 and 9 it can be noted that generally speaking, at the same nominal film Reynolds number the magnitudes of the tube averaged heat transfer coefficients of tube No. 1 to tube No. 5 decrease in order of the increasing tube number. This can be understood quite well because from top to down the amount of refrigerant liquid decreases in order, and we have found from Fig. 6 that with the decreasing in film Reynolds number the single tube heat transfer coefficient decreases. In all range of heat flux tested tube 5 is the lowest heat transfer coefficient because of the insufficient supply of liquid refrigerant.

As far as the effect of the film Reynolds number is concerned, for the case of heat flux of 10 kW/m^2 the HTCs of the five tubes decrease continuously from high film Reynolds number to lower one, showing convective heat transfer dominated character; while for the case of 20 kW/m^2 and beyond in the highest film Reynolds number region the increase trend of HTCs become mild and they even keep more or less constant, exhibiting nucleate boiling heat transfer dominated characteristics.

Come here to discuss the transition from full wetting region to partially dry-out region. For the case of 10 kW/m^2, the heat transfer coefficients of the five tubes show a trend of sudden decreasing at film Reynolds number about 600. When heat flux is low, the lower tubes can also receive enough falling liquid,hence their heat transfer behavior is more or less similar to tube No. 1. It should be noted that Jin et al. [17] obtained this transition Reynolds number about 350–400 under 40 kW/m^2 of R290 for smooth tube. This difference is reasonable because the enhanced tube has higher heat flux hence may goes into the dry-out regime at higher film flow rate.

With the increase in heat flux, because of the increased liquid evaporation rate at tube No. 1 the liquid falling to the subsequent tubes becomes less, and this may lead to partial dry-out of the lower tubes. For 20 kW/m^2, this transition can be observed for tube Nos. 4 and 5 at a higher film Reynolds number about 1000. Further increase in heat flux produces two effects: (1) making this transition Reynolds number of the lower tubes moves to higher value, (2) making more lower tubes having higher transition Reynolds number. As it can be seen from Fig. 11 this Reynolds number is about 1300 for tube Nos. 4 and 5, and from Fig. 12, transition occurs at this Reynolds number for tube Nos. 2,3,4 and 5. This difference can be attributed to the heat flux effect. At a higher heat flux, more liquid will be evaporated at the upper tubes, hence for lower tube even at higher nominal film Reynolds number, the liquid film has been already not enough to cover the entire tube surface, leading to partial dry-out.

The dry-out at low film flow rate may be resulted from two aspects. Firstly, uneven distribution of liquid refrigerant at lower film flow rate. Because the distributor is working under gravity, when the liquid flow rate is low, the liquid layer thickness in the distributor is thin, and the lack of stability of the surface may cause great liquid flow rate fluctuation between holes along the tube length. Secondly, the different heat transfer along the tube length. Water at the inlet has higher temperature and higher local heat transfer coefficient, leading to a higher local heat flux and evaporation rate.

Apart from the general variation trend mentioned above following two features can be noted.

The differences between HTCs of different tubes increase with heat flux. This phenomenon may be explained as follow. At the same nominal falling film Reynolds number of the five tubes, at a higher heat flux tube No. 1 will evaporate much more liquid, leading to an increase in heat transfer coefficient of tube No. 1 and a sharp decrease in the liquid which will further fall down to the lower tubes. The same situation happens at each tube, leading to a significant decrease in liquid falling on the lower tubes. It is because this reason that the HTC of tube No. 5 at heat flux of 40 kW/m^2 is averagely much less than those of three smaller heat fluxes.

At film Reynolds number about 600–2200 a very special variation of HTC with film Reynolds number happens for tube Nos. 4 and 5 at heat flux of 30 kW/m^2 and for all five tubes at heat flux of 40 kW/m^2, that is, the HTCs undulate, first decrease sharply with film Reynolds number, then increase again, and finally sharply decrease. We have repeated our test several times for confirming such a variation trend. A careful check of previous results reveal that such fluctuation of HTCs of falling film evaporation in tube bank has been found several times even though not so severe as shown by our test data. For example, in Fig. 11 of [5], and in Fig. 7 of [17] appreciable fluctuation can be observed.

This variation trend cannot be explained by conventional consideration. Thus we present here objectively to our heat transfer community for further study.

4.4. Heat transfer of tube No. 1

Since the nominal test conditions (film Reynolds number and heat flux) are the actual test conditions for the top tube in the tube bundle, it is interesting to show the effects of film Reynolds number and heat flux on the top tube heat transfer coefficient. The top tube performance at heat fluxes of 10, 20, 30 and 40 kW/m^2 is presented in Fig. 12 without the dry out part for clear presentation. As shown in Fig. 12, even though there is some bumpiness of test data for heat flux of 20 kW/m^2, the HTCs have following general variation trends: HTCs increase with film Reynolds number and heat flux. This implies that for the film evaporation of the top tubes both convective heat transfer and nucleate heat transfer both play their roles.

4.5. Comparisons between smooth and enhanced tube and R290 with R134a

Finally, we present the comparison among falling film heat transfer coefficients of No. 1 tube at 40 kW/m^2 of the present study for enhanced single enhanced tube and array with smooth tube [15] for R290 and the same enhanced tube array [14] for R134a in Fig. 13. We can find the following four points:

(1) The HTCs of enhanced single tube for R290 is higher than that of the smooth tube around 4.5 times.
(2) The HTCs of the enhanced tube array for R290 is higher than that of the smooth tube around 2.5 times.
(3) The HTCs of smooth tube are more uniform in the quasi-plateau stage than that of single and bundle enhanced tubes.
(4) The R290 HTCs of the tube array are higher than those of R134a for the same tube array in the plateau region by about 25%. This can be explained by the fact that the thermo-physical properties of R290 are more in favor of heat transfer than those of R 134a. The specific heat of R290 at T_s= 5.5 °C is almost twice than R134a and thermal conductivity almost 25% higher than R134a which lead to increase heat transfer rate of R 290 than R134a.

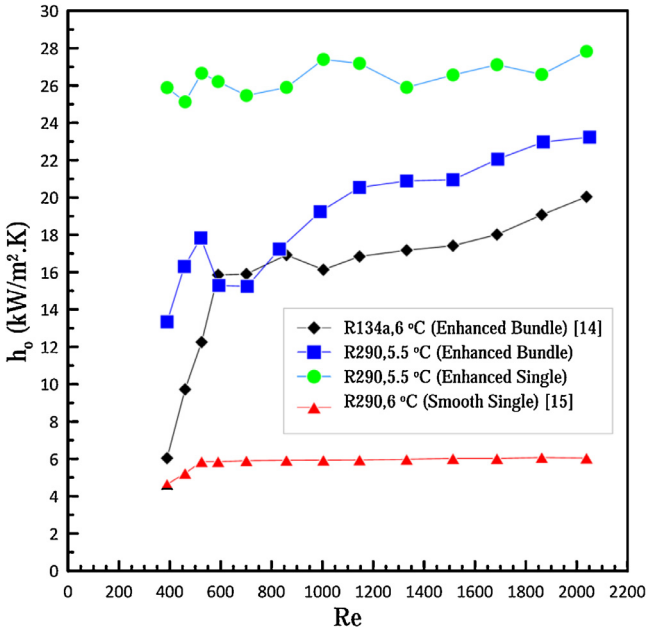

Fig. 13. Comparison among falling film heat transfer coefficients of the No. 1 tube at 40 kW/m^2 for enhanced single and array tubes with smooth tube [15] for R290 and enhanced bundle tube [14] for R134a.

It is to be noted that for the data compared in Fig. 13, there is minus difference in the saturation temperature (0.5 °C). Our previous study found that in the range of difference in several degrees saturation temperature have positive appreciable effect on the HTC of falling film evaporation [19], and 0.5 °C difference will not make much difference. In addition for the compared 134a its saturation temperature is higher than that of R 290 tube array test. Thus the compared results are in favor of R 134a.

5. Conclusions

Experiments have been carried out on heat transfer coefficients of falling film evaporators on horizontal enhanced single tube and tube array for R290, and following conclusions can be drawn:

(1) For R290 falling film evaporation on the enhanced tubes, with decrease of film flow rate the falling film heat transfer coefficients on the five tubes exhibit two general stages: at a larger film flow rate a plateau stage and at a smaller film flow rate a sharp drop stage.
(2) The falling film evaporation heat transfer coefficient on single enhanced tube is about 4.5 times of single smooth tube HTC, and the HTC of the enhanced tube array is higher than single smooth tube by more than 2.5 times. For the same enhanced tube array the HTCs of R290 are higher than those of R134a by about 25% in the plateau region.
(3) Heat flux has severe effect on the nominal film Reynolds number of lower tubes beyond which the partial dry-out occurs. For the case of 10 kW/m^2, the heat transfer coefficients of the five tubes shows a trend of sudden decreasing at film Reynolds number about 600. With the increasing in heat flux, because of the increased liquid evaporation rate at tube No. 1 the liquid falling to the subsequent tubes becomes less, leading to partial dry-out of the lower tubes. For 20 kW/m^2, this transition can be observed for tube Nos. 4 and 5 at a higher film Reynolds number about 1000. This Reynolds number is about 1300 for tube No. 4 and 5 at heat flux of 30 kW/m^2 and 40 kW/m^2, and when heat flux equal to 40 kW/m^2 transition occurs at this Reynolds number for tube Nos. 2, 3, 4 and 5. This is because at

a higher heat flux, more liquid will be evaporated at the upper tubes, hence for the lower tubes even at higher nominal film Reynolds number, the liquid film has been already not enough to cover the entire tube surface, leading to partial dry-out.

Author statement

All authors certify that they have participated sufficiently in the work to take public responsibility for the content, including participation in the concept, design, analysis, writing, or revision of the manuscript. Furthermore, each author certifies that this material or similar material has not been and will not be submitted to or published in any other publication before its appearance in the International Journal of Heat and Mass Transfer.

Declaration of Competing Interest

No conflict of interest needs to be declared.

Acknowledgments

Supports from Science Fund for Creative Research Groups of the National Natural Science Foundation of China (Grant no. 51721004) and from the 111 Project (B16038) are greatly acknowleged.

Supplementary materials

Supplementary material associated with this article can be found, in the online version, at doi:10.1016/j.ijheatmasstransfer.2020.120099.

References

[1] G. Ribatski, A.M. Jacobi, Falling-film evaporation on horizontal tubes—a critical review, Int. J. Refrig. 28 (5) (2005) 635–653.
[2] D. Gstohl, J. Thome, Visualization of R-134a flowing on tube arrays with plain and enhanced surfaces under adiabatic and condensing conditions, Heat Transf. Eng. 27 (10) (2006) 44–62.
[3] J.-.F. Roques, J. Thome, Falling films on arrays of horizontal tubes with R-134a, Part I: boiling heat transfer results for four types of tubes, Heat Transf. Eng. 28 (5) (2007) 398–414.
[4] J.F. Roques, J.R. Thome, Falling films on arrays of horizontal tubes with R-134a. Part II: flow visualization, onset of dry out, and heat transfer predictions, Heat Transf. Eng. 28 (5) (2007) 415–434.
[5] M. Habert, J.R. Thome, Falling-film evaporation on tube bundle with plain and enhanced tubes-Part I: experimental results, Exp. Heat Transf. 23 (2010) 259–280.
[6] M. Habert, J.R. Thome, Falling-film evaporation on tube bundle with plain and enhanced tubes-part II: new prediction methods, Exp. Heat Transf. 23 (2010) 281–297.
[7] L.H. Chien, Y.L. Tsai, An experimental study of pool boiling and falling film vaporization on horizontal tubes in R-245fa, Appl. Therm. Eng. 31 (2011) 4044–4054.
[8] M. Christians, J.R. Thome, Falling film evaporation on enhanced tubes, part 1: experimental results for pool boiling, onset-of-dry out and falling film evaporation, Int. J. Refrig. 35 (2) (2012) 300–312.
[9] M. Christians, J.R. Thome, Falling film evaporation on enhanced tubes, part 2: prediction methods and visualization, Int. J. Refrig. 35 (2012) 313–324.
[10] J. Fernández-Seara, Á.Á. Pardiñas, Refrigerant falling film evaporation review: description, fluid dynamics and heat transfer, Appl. Therm. Eng. 64 (1) (2014) 155–171.
[11] Ji Wen-Tao, Chuang-Yao Zhao, Ding-Cai Zhang, et al., Effect of vapor flow on the falling film evaporation of R134a outside a horizontal tube bundle, Int. J. Heat Mass Transf. 92 (2016) 1171–1181.
[12] C.Y. Zhao, W.T. Ji, P.H. Jin, W.Q. Tao, Heat transfer correlation of the falling film evaporation on a single horizontal smooth tube, Appl. Therm. Eng. 103 (2016) 177–186.
[13] C.Y. Zhao, P.H. Jin, W.T. Ji, Y.L. He, W.Q. Tao, Experimental investigations of R134a and R123 falling film evaporation on enhanced horizontal tube, Int. J. Refrig. 75 (2017) 190–203.
[14] C.Y. Zhao, W.T. Ji, P.H. Jin, Y.J. Zhong, W.Q. Tao, Experimental study of the local and average falling film evaporation coefficients in a horizontal enhanced tube bundle using R134a, Appl. Therm. Eng. 129 (2018) 502–511.
[15] P.H. Jin, C.Y. Zhao, W.T. Ji, W.Q. Tao, Experimental investigation of R410A and R32 falling film evaporation on horizontal enhanced tubes, Appl. Therm. Eng. 137 (2018) 739–748.
[16] P.H. Jin, Z. Zhang, I. Mostafa, C.Y. Zhao, W.T. Ji, W.Q. Tao, Heat transfer correlations of refrigerant falling film evaporation on a single horizontal smooth tube, Int. J. Heat Mass Transf. 133 (2019) 96–106.
[17] P.H. Jin, Z. Zhang, I. Mostafa, C.Y. Zhao, W.T. Ji, W.Q. Tao, Experimental study of falling film evaporation in tube bundles of doubly-enhanced, horizontal tubes, Appl. Therm. Eng. 170 (2020) 115006.
[18] S.M. Yang, W.Q. Tao, Heat Transfer, 4th edition, Higher Education Press, Beijing, China, 2006.
[19] V. Gnielinski, New equations for heat and mass transfer in the turbulent flow in pipes and channels, Int. Chem. Eng. 16 (1976) 359–368.
[20] W.T. Ji, C.Y. Zhao, D.C. Zhang, Z.Y. Li, Y.L. He, W.Q. Tao, Condensation of R134a outside single horizontal titanium, cupronickel (B10 and B30), stainless steel and copper tubes, Int. J. Heat Mass Transf. 77 (2014) 194–201.
[21] B. Cheng, W.Q. Tao, Experimental study of R-152a film condensation on single horizontal smooth tube and enhanced tubes, ASME J. Heat Transf. 116 (1994) 266–270.
[22] S.J. Kline, The purposes of uncertainty analysis, ASME J. Fluid Eng. 107 (1985) 153–160.
[23] Y.A. Cengel, A.J. Ghajar, Heat and Mass Transfer, Fundamentals and Applications, 4th ed., McGraw-Hill, 2011.